

## Radiative collisional quenching of metastable muonic hydrogen $p\mu^-(2s)$ and the metastable muonic helium ion $\alpha\mu^-(2s)$

James S. Cohen

*Physics Department, Rice University, Houston, Texas 77001*  
*and Theoretical Division, Los Alamos Scientific Laboratory, University of California, Los Alamos, New Mexico 87545*

J. N. Bardsley

*Physics Department, University of Pittsburgh, Pittsburgh, Pennsylvania 15260*

(Received 5 May 1980)

Fully quantum-mechanical calculations have been performed to determine the radiative collisional cross sections for quenching of metastable muonic hydrogen  $p\mu^-(2s)$  by normal hydrogen atoms and for quenching of the metastable muonic helium ion  $\alpha\mu^-(2s)$  by normal helium atoms. The interatomic potential curves and the radiative transition rates for the mixed electronic-muonic systems are calculated using molecular-structure methods. The nuclear motion is treated as adiabatic and the interaction is written in terms of a complex potential. The cross sections are evaluated by direct numerical integration of the Schrödinger equation. The two-body thermal (300 K) quenching rate constants obtained are  $3.7 \times 10^{-13}$  cm<sup>3</sup>/sec for  $p\mu^-$  and  $6.0 \times 10^{-13}$  cm<sup>3</sup>/sec for  $\alpha\mu^-$ .

### I. INTRODUCTION

The metastable muonic helium positive ion  $\alpha\mu^-(2s)$  has been obtained experimentally by stopping negative muons in gaseous helium.<sup>1</sup> There is also considerable interest in forming the 2s metastable state of muonic hydrogen, as yet unobserved.<sup>2</sup> Precise measurements on the  $n=2$  states by laser spectroscopy can provide important tests of quantum electrodynamics,<sup>3</sup> nuclear structure,<sup>4</sup> and possibly weak neutral-current effects.<sup>5</sup> Once formed, an isolated metastable muonic atom (or ion) lasts until destroyed by free-muon decay, two-photon radiation, or, much less likely, nuclear capture. The experiments are usually done in a dense gas however, so other deexcitation channels are available, mainly collision-induced radiation (Stark effect) and Auger ionization of an electron from another atom.<sup>1,6</sup> If these collisional quenching processes reduce the lifetime of the metastable species much below 1  $\mu$ sec, laser spectroscopy becomes considerably more difficult.<sup>1</sup> In fact, experiments with muonic helium have shown very little pressure dependence of the metastable lifetime at pressures between 7 and 50 atm (Ref. 1). Theory is in agreement that the external Auger process is unlikely,<sup>7</sup> but has predicted radiative quenching rates much faster than the experimental upper limit for muonic helium.

Mueller *et al.*<sup>8</sup> attributed this discrepancy to uncertainties in the values of the interatomic potential used in the calculations. The previous theoretical treatments, by Mueller *et al.*<sup>8</sup> and

Carboni and Pitzurra,<sup>9</sup> of radiative quenching of  $\alpha\mu^-(2s)$  in collisions with He have relied on the fact that the small muonic helium ion interacts with the electronic helium atom much as does a proton. The interatomic potential was thus taken to be the same as for the HeH<sup>+</sup> molecule and extrapolated by a Morse potential. In addition, they treated the adiabatic interaction perturbatively as linear Stark mixing between the 2s and 2p muonic atomic states; the effective electric field was determined by applying the Hellmann-Feynman theorem<sup>10</sup> with the HeH<sup>+</sup> interatomic potential. The above approximations seem reasonable, but we decided to eliminate them by determining the quasimolecular structure more directly since, as observed in both theoretical papers, the quenching rate is strongly dependent on the short-range interaction between the muonic helium ion and the helium atom.

As demonstrated by Mueller *et al.*,<sup>8</sup> the adiabatic description of thermal-energy collisions of  $\alpha\mu^-$  with He or  $p\mu^-$  with H is well justified. We determine the wave functions and potential energies in the Born-Oppenheimer approximation by describing the muon and electrons with basis set expansions and performing variational calculations. The transition moment as a function of internuclear distance is calculated with these wave functions. Using these results a complex potential is formed and the cross sections are evaluated quantum mechanically. The resulting rate for quenching of  $\alpha\mu^-(2s)$  in thermal collisions with the He atom is still much larger than that observed experimentally. We feel that this

strongly indicates that two-body collisions between the muonic helium ion and helium atoms are somehow precluded under the experimental conditions. Possible mechanisms for shielding muonic helium are mentioned in Sec. IV. It is important to observe that these mechanisms do not apply to the muonic hydrogen atom.

## II. INTERATOMIC INTERACTIONS

### A. Method

The quasimolecular structure calculations are done using a configuration-interaction code based on Slater-orbital nonorthogonal valence-bond configurations. To treat the muon consistently with the electrons, we modified the standard electronic-structure code<sup>11</sup> as follows: (i) The appropriate kinetic-energy operators are divided by the reduced mass of the muon ( $185.9m_e$  for  $p\mu^-$  and  $201.1m_e$  for  $\alpha\mu^-$ ), (ii) a new block for the muon is included in the Slater determinant,<sup>12</sup> and (iii) the Lamb shift is taken into account by a one-particle effective operator. In addition to these fundamental changes, care has to be exercised in the evaluation of integrals involving both muonic and electronic orbitals since the size of these orbitals typically differ enormously.

It will be noticed that in both the interactions of concern here,  $p\mu^-$  with H and  $\alpha\mu^-$  with He, the nuclei of the interacting atoms are identical. In principle, this implies that the wave functions should be required to have inversion symmetry. However, since the overlap of a muonic orbital on one nucleus with a similar orbital on the other nucleus is negligible at internuclear distances  $R$  of the order of  $1a_0$ , the effect of this symmetry on the wave function is also negligible except at very small  $R$ . In thermal collisions between  $\alpha\mu^-$  and He such close approaches are prevented by the Coulomb barrier. On the other hand, since  $p\mu^-$  is neutral, muonic hydrogen can approach a hydrogen nucleus to within a distance of a few  $a_\mu$  ( $1a_\mu \approx 0.005a_0$ ), where inversion symmetry does play a significant role. Nevertheless the effect on the radiative collision cross section is very small.

### B. Interaction of $p\mu^-$ with H

A schematic diagram of the energy levels of muonic hydrogen is given in Fig. 1. In the calculations the fine and hyperfine structure splittings are ignored, leaving the average shift of the  $2s$  level relative to the  $2p$  level, taken as  $-0.0075$  a.u. This splitting is introduced by an effective operator which gives zero except when acting on muonic  $s$  orbitals. The wave function consists

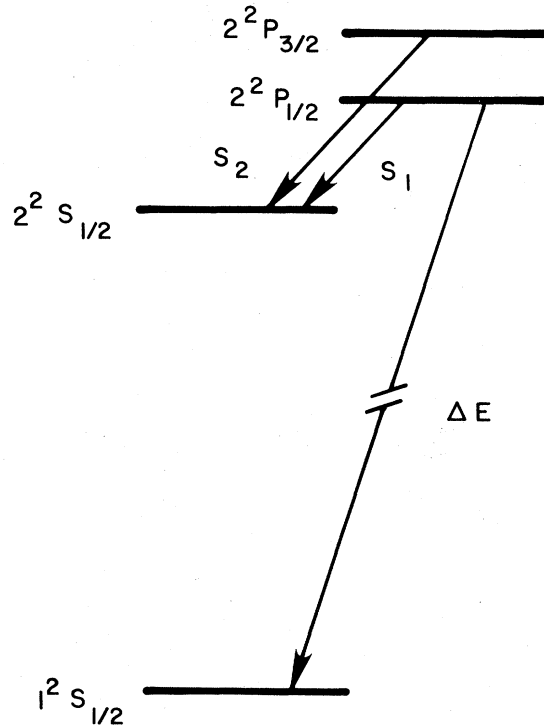


FIG. 1. Schematic diagram of energy levels. In muonic hydrogen ( $p\mu^-$ ),  $S_1=0.21$  eV,  $S_2=0.22$  eV, and  $\Delta E=1.9$  keV. For the muonic helium ion ( $\alpha\mu^-$ ),  $S_1=1.38$  eV,  $S_2=1.53$  eV, and  $\Delta E=8.2$  keV. The hyperfine structure is not shown. [See V. W. Hughes and T. Kinoshita, in *Muon Physics*, edited by V. W. Hughes and C. S. Wu (Academic, New York, 1977), Vol. I, pp. 124-127.]

of four terms:  $1s_{ea}1s_{\mu b}$ ,  $1s_{ea}1s'_{\mu b}$ ,  $1s_{ea}2s_{\mu b}$ , and  $1s_{ea}2p_{\mu b}$ , where  $a$  or  $b$  designates the nuclear center,  $e$  or  $\mu$  designates electronic or muonic, and a prime distinguishes a second orbital of the same quantum numbers but different exponents. Trial calculations were performed in which the orbital exponents were optimized, additional electronic orbitals were added, or inversion symmetry was enforced. These tests showed that the four-term wave function with hydrogenic orbitals is adequate for  $R \geq 0.2a_0$ .

The second lowest eigenvalue in the variational calculation corresponds to the adiabatic interaction of  $p\mu^-$  ( $2s$ ) with H. The electric-dipole transition moment  $\vec{\mu}(R)$  connecting this state with the adiabatic ground state was calculated using the variational wave functions. The transition moments computed in the length and velocity formulations agree to 3 or 4 significant figures. The results for the interatomic potential energy  $V$ , the energy difference  $\Delta E$  between the two adiabatic states, and the transition moment  $\mu$  are

given as a function of  $R$  in Table I. In addition, the transition rate at fixed  $R$ , which is given by the Einstein  $A$  coefficient

$$A(R) = \frac{4g}{3c^3} [\Delta E(R)]^3 |\vec{\mu}(R)|^2, \quad (1)$$

where  $c$  is the velocity of light and the degeneracy  $g$  is 1 here, is listed. The potential curve and transition rate are plotted in Fig. 2. At  $R \geq 2a_0$ , the values of  $\mu$  and  $A$  decrease nearly exponentially with  $R$ , as the charge of the hydrogen nucleus becomes better shielded by the electronic charge cloud.

At  $R < 0.1a_0$  the potential was taken as the average of those obtained enforcing gerade and ungerade inversion symmetry (the resulting curve has a minimum at  $R \approx 0.08a_0$ ). The cross section is insensitive to the potential at such small  $R$  so this approximation is quite adequate.

### C. Interaction of $\alpha\mu^-$ with He

To a good first approximation the interatomic potential of  $\alpha\mu^- + \text{He}$  is just that of  $\text{HeH}^+$  in the thermally accessible region. Hence the first step was to obtain a good small wave function for this simple molecule. The  $\text{HeH}^+$  wave function chosen consists of nine terms of  $^1\Sigma$  symmetry,

$$\begin{aligned} \psi(\text{HeH}^+) = & c_1(1s_{\text{He}})^2 + c_2(2s_{\text{He}})^2 + c_3(1s_{\text{He}} 2s_{\text{He}}) \\ & + c_4(2p_{\text{He}}^x)^2 + c_5(2p_{\text{He}}^y)^2 + c_6(1s_{\text{He}} 2p_{\text{He}}^x) \\ & + c_7(1s_{\text{He}}' 1s_{\text{H}}) + c_8(1s_{\text{He}}' 2s_{\text{H}}) + c_9(1s_{\text{He}}' 2p_{\text{He}}^x). \end{aligned} \quad (2)$$

The orbital exponents were optimized at each internuclear distance considered. Near the minimum  $R_e$  of the potential curve, the values

TABLE I. Interaction of  $p\mu^-$  with H.

| $R(a_0)^a$ | $V(\text{a.u.})^b$ | $\Delta E(\text{a.u.})$ | $\mu(\text{a.u.})^c$   | $A(\text{a.u.})$       |
|------------|--------------------|-------------------------|------------------------|------------------------|
| 0.1        | -1.790 756         | 67.92                   | $3.042 \times 10^{-3}$ | $1.50 \times 10^{-6}$  |
| 0.2        | -0.419 039         | 69.29                   | $2.912 \times 10^{-3}$ | $1.46 \times 10^{-6}$  |
| 0.4        | -0.095 342         | 69.62                   | $2.821 \times 10^{-3}$ | $1.39 \times 10^{-6}$  |
| 0.6        | -0.036 781         | 69.68                   | $2.725 \times 10^{-3}$ | $1.30 \times 10^{-6}$  |
| 0.8        | -0.016 760         | 69.70                   | $2.578 \times 10^{-3}$ | $1.17 \times 10^{-6}$  |
| 1.0        | -0.007 999         | 69.70                   | $2.347 \times 10^{-3}$ | $9.66 \times 10^{-7}$  |
| 1.2        | -0.003 763         | 69.71                   | $2.005 \times 10^{-3}$ | $7.06 \times 10^{-7}$  |
| 1.4        | -0.001 697         | 69.71                   | $1.571 \times 10^{-3}$ | $4.33 \times 10^{-7}$  |
| 1.6        | -0.000 736         | 69.71                   | $1.129 \times 10^{-3}$ | $2.24 \times 10^{-7}$  |
| 1.8        | -0.000 315         | 69.71                   | $7.639 \times 10^{-4}$ | $1.02 \times 10^{-7}$  |
| 2.0        | -0.000 136         | 69.71                   | $5.023 \times 10^{-4}$ | $4.43 \times 10^{-8}$  |
| 2.5        | -0.000 019         | 69.71                   | $1.717 \times 10^{-4}$ | $5.17 \times 10^{-9}$  |
| 3.0        | -0.000 004         | 69.71                   | $5.939 \times 10^{-5}$ | $6.19 \times 10^{-10}$ |

<sup>a</sup>  $1a_0 = 0.52918 \times 10^{-8}$  cm.

<sup>b</sup> 1 a.u. = 27.212 eV.

<sup>c</sup> 1 a.u. (electric dipole moment) = 2.542 D.

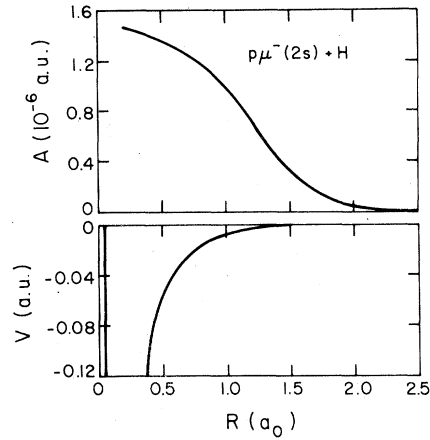


FIG. 2. Potential energy and radiative transition rate for  $p\mu^-(2s) + \text{H}$  as a function of internuclear distance.

of the exponents are  $\alpha(1s_{\text{He}}) = 2.43$ ,  $\alpha(1s'_{\text{He}}) = 1.94$ ,  $\alpha(2s_{\text{He}}) = 1.98$ ,  $\alpha(2p_{\text{He}}^x) = 2.77$ ,  $\alpha(2p_{\text{He}}^y) = 2.58$ ,  $\alpha(1s_{\text{H}}) = 1.19$ ,  $\alpha(2s_{\text{H}}) = 1.19$ , and  $\alpha(2p_{\text{H}}^x) = 1.86$ . The dissociation energy obtained is 1.995 eV, to be compared with the very accurate theoretical value<sup>13</sup> 2.04 eV and the experimental value<sup>14</sup>  $2.0 \pm 0.1$  eV. The potential curve was found to be attractive at all  $R > R_e$ .

The relevant energy levels of the muonic helium ion are given in Fig. 1. The average  $2s-2p$  splitting, 0.054 a.u., is taken into account in the same manner as for muonic hydrogen. A 36-term wave function for  $p\mu^- + \text{He}$  is formed by replacing the hydrogen nucleus in  $\text{HeH}^+$  by a helium nucleus with a muonic orbital,  $1s_{\mu}$ ,  $1s'_{\mu}$ ,  $2s_{\mu}$ , or  $2p_{\mu}$ . As before, the muonic orbital exponents are taken as hydrogenic (with  $Z=2$  here). The adiabatic interaction between  $\alpha\mu^-(2s)$  and He is given by the tenth eigenvalue in the variational calculation. The dipole transition moment between this state and the ground state was calculated in the length and velocity formulations and the two are in good agreement as in the case of  $p\mu^- + \text{H}$ . The results for  $V$ ,  $\Delta E$ ,  $\mu$ , and  $A$  are given in Table II. It may be observed that the dipole transition matrix element changes sign near the minimum of the potential curve. This behavior can be interpreted as a result of the Stark electric field changing direction; for example, if the Hellmann-Feynman theorem<sup>10</sup> is assumed then the electric field along the internuclear axis is

$$E \approx \frac{1}{e} \frac{dV(R)}{dR}. \quad (3)$$

The transition rate is so small at  $R \geq R_e$  that the change of sign is of only academic interest. The potential curve and transition rate are plotted in Fig. 3. At a given internuclear distance the ma-

TABLE II. Interaction of  $\alpha\mu^-$  with He.

| $R(a_0)$ | $V(\text{a.u.})$ | $\Delta E(\text{a.u.})$ | $\mu(\text{a.u.})$      | $A(\text{a.u.})$       | $\Delta V^a(\text{a.u.})$ |
|----------|------------------|-------------------------|-------------------------|------------------------|---------------------------|
| 0.1      | 14.241 38        | 300.12                  | $1.337 \times 10^{-3}$  | $2.50 \times 10^{-5}$  | -1.526 15                 |
| 0.3      | 2.917 31         | 301.53                  | $1.193 \times 10^{-3}$  | $2.02 \times 10^{-5}$  | -0.122 09                 |
| 0.5      | 0.942 95         | 301.63                  | $8.712 \times 10^{-4}$  | $1.08 \times 10^{-5}$  | -0.026 31                 |
| 0.7      | 0.304 21         | 301.65                  | $4.490 \times 10^{-4}$  | $2.87 \times 10^{-6}$  | -0.004 28                 |
| 0.9      | 0.059 90         | 301.65                  | $1.895 \times 10^{-4}$  | $5.11 \times 10^{-7}$  | -0.001 00                 |
| 1.0      | 0.000 95         | 301.65                  | $1.188 \times 10^{-4}$  | $2.01 \times 10^{-7}$  | -0.000 56                 |
| 1.1      | -0.035 21        | 301.65                  | $7.192 \times 10^{-5}$  | $7.36 \times 10^{-8}$  | -0.000 36                 |
| 1.2      | -0.056 43        | 301.65                  | $4.088 \times 10^{-5}$  | $2.38 \times 10^{-8}$  | -0.000 26                 |
| 1.3      | -0.067 78        | 301.65                  | $2.048 \times 10^{-5}$  | $5.96 \times 10^{-9}$  | -0.000 19                 |
| 1.4      | -0.072 65        | 301.65                  | $6.973 \times 10^{-6}$  | $6.91 \times 10^{-10}$ | -0.000 16                 |
| 1.4632   | -0.073 43        | 301.65                  | $9.361 \times 10^{-7}$  | $1.25 \times 10^{-11}$ | -0.000 14                 |
| 1.5      | -0.073 28        | 301.65                  | $-1.822 \times 10^{-6}$ | $4.72 \times 10^{-11}$ | -0.000 13                 |

$$^a \Delta V = V(\text{He} + \alpha\mu^-) - V(\text{He} + \text{H}^+).$$

trix element  $\mu$  tends to be smaller for helium than for hydrogen, mainly because of the larger Lamb shift in helium; this effect is opposed in the transition rate  $A$  by the larger transition energy  $\Delta E$  of muonic helium. The difference  $\Delta V$  between the interatomic potential energies of  $\text{He} + \alpha\mu^-(2s)$  and  $\text{He} + \text{H}^+$  is also given in Table II. In the thermally accessible region the potential curve of  $\text{HeH}^+$  approximates that of  $\text{He} + \alpha\mu^-$  to within about 0.02 eV.

### III. RADIATIVE COLLISIONAL CROSS SECTIONS

The radiative decay of the adiabatic state formed in the interaction of the metastable muonic atom (or ion) with the normal atom can be described quantum mechanically by a complex potential<sup>15</sup>

$$W(R) = V(R) - \frac{1}{2}i\hbar A(R). \quad (4)$$

Scattering by this potential results in complex

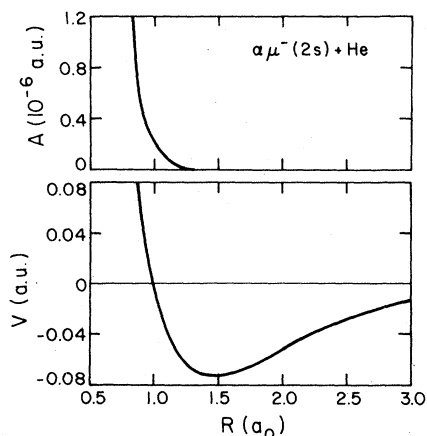


FIG. 3. Potential energy and radiative transition rate for  $\alpha\mu^-(2s) + \text{He}$  as a function of internuclear distance.

partial-wave phase shifts

$$\eta_l = \eta_l^R + i\eta_l^I. \quad (5)$$

The cross section for a radiative transition is then given by

$$\sigma = \frac{\pi}{k^2} \sum_l (2l+1)(1 - e^{-4\eta_l^I}), \quad (6)$$

in which  $k$  is the wave number corresponding to the relative motion of the nuclei. The sum extends over all integral values of  $l$  since we have ignored nuclear symmetry. The phase shifts were evaluated both in the JWKB approximation and by direct numerical integration of the partial-wave equations

$$\left( \frac{d^2}{dR^2} + k^2 - \frac{l(l+1)}{R^2} - 2MW(R) \right) u_l(R) = 0. \quad (7)$$

For collisions of  $\alpha\mu^-$  with He the semiclassical approximation is adequate. However, for collisions of  $p\mu^-$  with H the fully quantum-mechanical treatment is preferable since orbiting resonances contribute significantly to the low-energy scattering.

The radiative transition cross sections are shown in Figs. 4 and 5 for  $p\mu^-$  and  $\alpha\mu^-$ , respectively. The structure exhibited by the cross sections at low collision energy is due principally to the effects of the centrifugal barriers and a given peak can generally be associated with a single partial wave. Of particular importance are the prominent orbiting resonances in the cross sections for  $p\mu^- + \text{H}$ , which may be expected to dominate thermal scattering.

The collisions of  $p\mu^-$  with H and  $\alpha\mu^-$  with He are qualitatively different in one respect. As can be observed from Fig. 2, very close collisions between  $p\mu^-$  and H can occur even near zero energy, so that the quenching occurs in the region

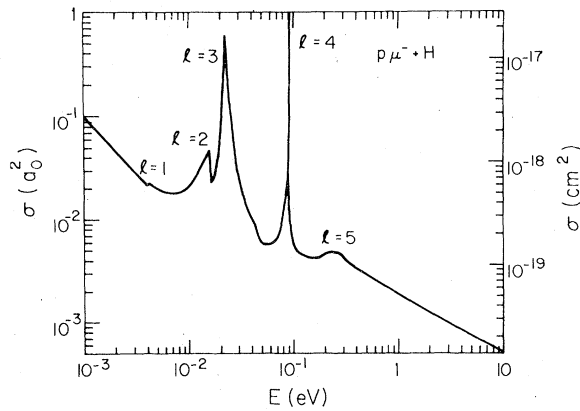


FIG. 4. Radiative quenching cross section for collisions of  $p\mu^-(2s)$  with H as a function of center-of-mass energy. The peaks due to  $l=0$  to 5 are labeled.

where the transition rate  $A$  is not a strong function of  $R$ . Consequently, except near energies where orbiting can occur, the cross section tends to decrease with increasing collision energy simply because the system spends less time in the strong transition region. On the other hand, it may be observed from Fig. 3 that the nuclear repulsion between  $\alpha\mu^-$  and He requires quenching of  $\alpha\mu^-$  in thermal collisions to occur at distances where the transition rate decreases rapidly as  $R$  increases, i.e., at distances where the nucleus of He is still significantly shielded by its electrons. Consequently, the quenching occurs almost completely near the classical turning point. This distance is small enough that radiation still occurs in low-energy collisions and the low-energy behavior of the cross section is similar to that for  $p\mu^- + H$ . However, at  $E \approx 2$  eV the cross section begins slowly to rise again as the ion penetrates to dis-

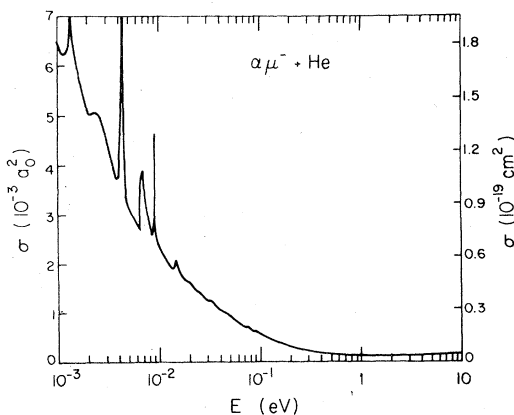


FIG. 5. Radiative quenching cross section for collisions of  $\alpha\mu^-(2s)$  with He as a function of center-of-mass energy.

tances where the transition rate is considerably larger (it peaks at  $E \approx 60$  eV). Of course, this behavior may not actually be seen since in all of the present calculations we have ignored inelastic channels. The  $2s \rightarrow 2p$  inelastic excitation<sup>16</sup> becomes energetically possible at a center-of-mass collision energy of 0.2 eV for  $p\mu^- + H$  and 1.4 eV for  $\alpha\mu^- + He$ . Under experimental conditions it appears that energy loss is fast enough to slow a significant fraction of the muonic atoms to kinetic energies below the inelastic threshold<sup>17</sup> even in the case of  $p\mu^-$ .

#### IV. DISCUSSION

Our cross section for  $p\mu^-(2s) + H$  is somewhat larger than that obtained by Mueller *et al.*<sup>8</sup> We found that the fully quantum-mechanical treatment is required in order to treat accurately the shape resonances which dominate thermal-energy scattering in hydrogen. For  $\alpha\mu^-(2s) + He$  our quantal and semiclassical results are in close agreement. However, the cross section is about an order of magnitude larger than the "quantum-mechanical" result of Mueller *et al.* and about a factor of 3 larger than their "classical-path" result. We do not know the source of either the large discrepancy with our calculation or the large difference between the two results of Mueller *et al.*, but we suspect numerical errors in their work.

The radiative collisional cross sections presented in Sec. III imply thermal (300 K) rate constants of  $3.7 \times 10^{-13}$  cm<sup>3</sup>/sec for quenching of  $p\mu^-(2s)$  by H and  $6.0 \times 10^{-15}$  cm<sup>3</sup>/sec for quenching of  $\alpha\mu^-(2s)$  by He (the corresponding average cross sections are  $1.1 \times 10^{-18}$  and  $3.4 \times 10^{-20}$  cm<sup>2</sup>, respectively). In principle, these rates should be lower limits on the total quenching rates for the two-body collisions. Additional quenching may occur via formation of a bound molecule,<sup>9,18</sup> ( $He\alpha\mu^-$ )<sup>+</sup> or  $Hp\mu^-$ . However, the rate obtained here for quenching of  $\alpha\mu^-(2s)$  in collisions with helium atoms is already much larger than the experimentally placed upper limit.<sup>1</sup> Since we have avoided approximations made in previous calculations and still obtain a quenching rate much larger than observed, we conclude that two-body collisions between  $\alpha\mu^-$  and He must not freely occur under the experimental conditions (pressures between 7 and 50 atm). One mechanism for preventing radiative collisions would be neutralization of the muonic helium ion by addition of an electron. The interatomic potential curve would then be like that of HeH which is repulsive, except for a long-range van der Waals well, and the Stark mixing at the distance of closest approach would

be extremely small. However, there are two problems with this mechanism: (i) The electron is not readily available since the ionization potential of He is greater than that of  $\alpha\mu^-e$ , and (ii) the internal Auger process would occur at a rate  $1.70 \times 10^8$ /sec (obtained using the theory of Burbidge and de Borde<sup>19</sup>). This is slow for an internal Auger rate but still much faster than the observed quenching rate. A more likely mechanism for preventing radiative collisions is by formation of a cluster of helium atoms about the muonic helium ion as discussed by Bertin *et al.*<sup>1</sup>

If the atoms are symmetrically placed about the ion, there is no net Stark mixing in first order. Note that neither of these mechanisms would apply to muonic hydrogen since  $p\mu^-$  is a neutral species. Experiments with  $p\mu^-(2s)$  at high pressures may still have to contend with the theoretically predicted short lifetime.

#### ACKNOWLEDGMENT

This work was performed under the auspices of the U. S. Department of Energy.

- 
- <sup>1</sup>A. Bertin, G. Carboni, A. Placci, E. Zavattini, U. Gastaldi, G. Gorini, G. Neri, O. Pitzurra, E. Polacco, G. Torelli, A. Vitale, J. Duclos, and J. Picard, *Nuovo Cimento* **26B**, 433 (1975).
- <sup>2</sup>H. Anderhub, H. Hofer, F. Kottmann, P. LeCoultré, D. Makowiecki, O. Pitzurra, B. Sapp, P. G. Seiler, M. Wälchli, D. Taqqu, P. Truttmann, A. Zehnder, and C. Tschalär, *Phys. Lett.* **71B**, 443 (1977); P. O. Egan, V. W. Hughes, D. C. Lu, F. Mariam, P. A. Souder, J. Vetter, G. zu Putlitz, A. B. Denison, C. Grassl, and P. A. Thompson, *Bull. Am. Phys. Soc.* **23**, 577 (1978); G. Fiorentini and O. Pitzurra, *Nuovo Cimento* **43A**, 396 (1978).
- <sup>3</sup>A. Di Giacomo, *Nucl. Phys.* **B11**, 411 (1969); E. Campani, *Lett. Nuovo Cimento* **4**, 512 (1970); **4**, 982 (1970).
- <sup>4</sup>J. Bernabeu and C. Jarlskog, *Nucl. Phys.* **E75**, 59 (1974); *Phys. Lett.* **60B**, 197 (1976); E. M. Henley, F. R. Krejs, and L. Wilets, *Nucl. Phys.* **A256**, 349 (1976); G. A. Rinker, *Phys. Rev. A* **14**, 18 (1976).
- <sup>5</sup>J. Bernabeu, T. E. O. Ericson, and C. Jarlskog, *Phys. Lett.* **50B**, 467 (1974).
- <sup>6</sup>G. Gorini and G. Torelli, *Lett. Nuovo Cimento* **13**, 517 (1975).
- <sup>7</sup>M. Leon and H. A. Bethe, *Phys. Rev.* **127**, 636 (1962).
- <sup>8</sup>R. O. Mueller, V. W. Hughes, H. Rosenthal, and C. S. Wu, *Phys. Rev. A* **11**, 1175 (1975).
- <sup>9</sup>G. Carboni and O. Pitzurra, *Nuovo Cimento* **25B**, 367 (1975).
- <sup>10</sup>J. O. Hirschfelder and W. J. Meath, in *Intermolecular Forces*, edited by J. O. Hirschfelder (Interscience, New York, 1967), p. 53.
- <sup>11</sup>Computer code of J. C. Browne, University of Texas Molecular Physics Group.
- <sup>12</sup>F. Prosser and S. Hagstrom, *Int. J. Quantum Chem.* **2**, 89 (1968).
- <sup>13</sup>L. Wolniewicz, *J. Chem. Phys.* **43**, 1087 (1965); W. H. Miller and H. F. Schaefer, *ibid.* **53**, 1421 (1970).
- <sup>14</sup>H. P. Weise, H. U. Mittmann, A. Ding, and A. Henglein, *Z. Naturforsch.* **26a**, 1122 (1971).
- <sup>15</sup>J. S. Cohen and J. N. Bardsley, *Phys. Rev. A* **18**, 1004 (1978).
- <sup>16</sup>G. Kodosky and M. Leon, *Nuovo Cimento* **1B**, 41 (1971).
- <sup>17</sup>G. Carboni and G. Fiorentini, *Nuovo Cimento* **39B**, 281 (1977).
- <sup>18</sup>J. E. Russell, *Phys. Rev. A* **18**, 521 (1978).
- <sup>19</sup>G. R. Burbidge and A. H. de Borde, *Phys. Rev.* **89**, 189 (1953).